

Encapsulation of *p*-Acetylarsenazo in Nanoscale MCM-41

MING-QIANG ZOU¹, YU XUE² and QING-ZHOU ZHAI^{2*}

¹Chinese Academy of Inspection and Quarantine, Beijing 100023, P.R. China

²Research Center for Nanotechnology, Changchun University of Science and Technology, 7186 Weixing Road, Changchun 130022, Jilin Province, P.R. China

*Corresponding author: Fax: +86 431 85383815; Tel: +86 431 85583118; E-mail: zhaiqingzhou@163.com; zhaiqingzhou@hotmail.com

(Received: 11 August 2010;

Accepted: 22 December 2010)

AJC-9416

MCM-41 molecular sieve was prepared in alkaline medium by using cetyltrimethylammonium bromide as template, tetraethoxysilane (TEOS) as silica resource. Guest material *p*-acetylarsenazo (ASApA) was incorporated into the molecular sieve host to obtain host-guest nanocomposite materials (MCM-41)-ASApA. Chemical analysis showed that *p*-acetylarsenazo has entered in the MCM-41 host. The powder X-ray diffraction test results indicated that the ordered degrees of the MCM-41 in the host-guest nanocomposite materials were still remained good and the frameworks of the molecular sieves were not destroyed by the incorporation of the *p*-acetylarsenazo. The low-temperature nitrogen adsorption-desorption results at 77 K showed that the surface area and the pore volume of the post-encapsulation host-guest nanocomposite materials were decreased compared to those of the unincorporated host molecular sieves, indicating that the guest has partially occupied the channels of the molecular sieves. The scanning electron microscopic studies indicated that the (MCM-41)-ASApA particles presented spherical and have a size of 115 ± 10 nm for the sample containing 2.93 % of *p*-acetylarsenazo. Raman spectra showed that the frameworks of the host molecular sieves of the prepared host-guest nanocomposite materials were kept intact. The ultraviolet-visible solid state diffuse reflection absorption spectra indicated that the absorptions of the host-guest nanocomposite materials prepared had obvious blue-shifts compared with that of the guest material, proving that the guest dye had already incorporated into the channels of the molecular sieves. The luminous spectra showed that the post-encapsulation host-guest composite materials have the character of luminescence at 466 nm. The host-guest composite materials (MCM-41)-ASApA have potential use in the domain of sensor, light-emitting devices and laser part materials.

Key Words: *p*-Acetylarsenazo, MCM-41, Nanocomposite material, Host-guest material.

INTRODUCTION

Kresge *et al.*¹, reported an ordered mesoporous material, namely MCM-41. The material has hexagonal orderly arranged pore channels with uniform size, whose pore size can be continuously adjusted within the scope of 2 to 20 nm. It has received wide attention from the general scientific researchers. In addition, its excellent structural property and simple preparation process have promised great potential in many areas. Since its regular nano-pore channels can increase the specific surface area of catalyst and this leads to greatly increase efficiency of the catalyst in the reaction^{2,3}, it can be served as a good catalyst carrier in the chemical field. Moreover, MCM-41 molecular sieves have also been applied to the degradation of organic dyes, such as rhodamine B⁴ and to the separation of mixture of low-carbon alcohol and water⁵. Organic dye molecules have strong singlet-singlet transitions, promising great potential for application in the spectrophotometric measurement, solid dye

lasers and spectroscopy, *etc.*⁶⁻⁹. However the commonly used organic dyes are dispersed in liquid medium. Since organic dye molecules can not avoid the occurrence of reunion in solutions, stimulated energy of molecules will be lost by thermal relaxation vibration, which leads to the disability of reflecting luminescence in many cases. Cai *et al.*¹⁰ synthesized nano-MCM-41 molecular sieve for the first time. Since then, no reports on further theoretical and application researches of nano-MCM-41 have been established yet. On a nano-scale, to hybridize series of materials by using organic or inorganic molecules can generate composite materials with new features.

p-Acetylarsenazo (ASApA), *i.e.* [2-(2-arsenic phenylazo)-7-(4-acetyl-phenylazo)-1,8-dihydroxy-3,6-naphthalene disulfonic acid], is an organic dye (Fig. 1). *p*-Acetylarsenazo is able to have colour reaction with certain metal ions, which will produce complex compound. In addition, its antiinterference ability and stability are both outstanding, which can be utilized in measuring metal content¹¹.

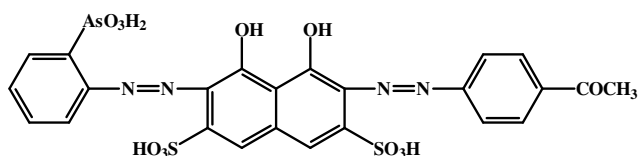


Fig. 1. Molecular structure of *p*-acetylarsenazo

In recent years, as the study of nanocomposite materials is ascending endlessly into a hot issue, mesoporous MCM-41 molecular sieve has again becomes an ideal host platform for host-guest nanocomposite materials, among which the object materials can be metal, inorganic molecules, organic dyes, *etc.* Xu *et al.*¹² assembled europium and fluorescent dye eosin Y, as the guest in the pores of MCM-41 host, getting the assembly of composite Eosin Y/Eu-MCM-41 mesoporous materials. Chen *et al.*¹³ successfully loaded laser dye coumarin 151 to MCM-41 powder with a mesoporous structure through the method of crystal coating and prepared powder and fiber materials with the feature of photoluminescence. However, none refers to *p*-acetylarsenazo.

In this study, nano-MCM-41 molecular sieve is taken as the main body. Meanwhile, (MCM-41)-ASApA host-guest composite materials are prepared. This study characterized the prepared nanocomposite materials using chemical analysis, X-ray diffraction, N₂ adsorption-desorption, scanning electron microscopy, Raman spectroscopy, UV-visible solid diffuse reflection absorption spectroscopy and luminescence study. Results show that *p*-acetylarsenazo has been successfully assembled into nanopores of MCM-41 molecular sieves. The host-guest composite materials have a feature of luminescent property, promising potential use in the domain of sensor, light-emitting devices and laser part materials.

EXPERIMENTAL

p-Acetylarsenazo (Changke Institute of Chemical Reagents, Jinsheng Chemical Corp., Ltd, China); Cetyltrimethyl ammonium bromide (CTMAB, AR, Shanghai Reagent Factory, Sinopharmaceutical Medicine Group, China); Tetraethyl-orthosilicate (TEOS, AR, Shanghai Chemical Pharmaceutical Co., Ltd., China); Sodium hydroxide (AR, Beijing Chemical Factory, China) and deionized water.

The silica content of the sample was measured by the siliconantimomolybdate heteropoly blue photometry¹⁴ using 722S spectrophotometer and *p*-acetylarsenazo content was obtained by difference. Powder X-ray diffraction spectrogram was detected by D5005 diffractometer (Germany Siemens). CuK_α target was used for the measurement to get data with the following operation parameters: X-ray wavelength of 0.154 nm, tube voltage of 30 kV, tube current of 20 mA, 2θ value from 0.4-10.0°, step length of 0.02°. Low temperature N₂ adsorption-desorption studies: The surface area and pore volume of the sample were determined in the Micromeritics ASAP2010M adsorption meter (the US Mike Company) at 77 K, the sample was firstly vacuumed and activated at 573 K for 12 h. The data were calculated according to model BdB (Broekhoff and de Boer)¹⁵. By Brunner-Emmett-Teller (BET) method¹⁶, the sample surface area was measured. By (Barrett-Joyner-Halenda (BJH) method, the pore structure was analyzed.

Scanning electron microscopy (SEM) was scanned by Japanese Jeol JSM-5600L scanning electron microscope, before the observation, the sample was treated by adopting a higher secondary electron emission coefficient for metal plating of conductive layer. Raman spectra of samples were determined by Portable Raman Detector (Optotrace Technologies Inc., USA), getting excitation wavelength of 785 nm, continuous output power of 200 mW and measurement range between 1200-200 cm⁻¹. UV-Visible solid diffuse reflection spectra: by the application of Japan's Hitachi Electric Company U-4100 UV spectrophotometer, the matrix was set as α-Al₂O₃ with the measuring range of 200-800 nm. The fluorescence spectroscopic measurement was completed on the SPEX-FL-2T-2 double-grating fluorescence spectrometer (SPEX Company, USA) at room temperature of 20 °C.

Preparation of nanometer MCM-41 molecular sieve: Firstly, 480 mL of distilled water was combined with 1.0 g of cetyltrimethyl ammonium bromide at constant temperature of 80 °C. It was strongly stirred until the solution became homogeneous and then 3.5 mL of 2 mol/L NaOH solution was added. 5 mL of tetraethylorthosilicate was added slowly after stirring evenly. Its reaction should be lasting for 2 h at 80 °C; then the solution was filtered and the obtained products were washed with distilled water, dried at room temperature. Finally the sample powder was put into a muffle furnace at 500 °C burning for 4 h, generating nanometer MCM-41 mesoporous molecular sieve with the appearance of white powder.

Preparation of host-guest nanocomposite material (MCM-41)-ASApA: The nano-MCM-41 molecular sieve was dehydrated at 200 °C for 3 h. Two of the above-mentioned nano-MCM-41 molecular sieves (0.300 g for each) were, respectively, placed in 30 mL of ASApA aqueous solution with the concentrations of 5.0 × 10⁻³ and 5.0 × 10⁻⁴ mol/L. They were stirred in 50-mL beakers at a room temperature of 20 °C for 48 h. The obtained products were filtered and carefully and repeatedly washed with deionized water until getting colourless filtrate. At the temperature of 60 °C, the products were placed for a fraction for 6 h. Then, host-guest nanocomposite materials (MCM-41)-ASApA were generated. The sample made from ASApA aqueous solution of lower concentration (5.0 × 10⁻⁴ mol/L) was marked as (MCM-41)-ASApA-(I), while the one made from ASApA aqueous solution of higher concentration (5.0 × 10⁻³ mol/L) was marked as (MCM-41)-ASApA-(II).

RESULTS AND DISCUSSION

The contents of silica in the host-guest composite material samples were determined by the siliconantimomolybdate heteropoly blue photometry¹⁴ and the amount of ASApA calculated by difference. Chemical analysis showed that the two samples (MCM-41)-ASApA-(I) and (II) prepared contained 0.82, 2.93 % of ASApA, respectively. This showed that the ASApA have been incorporated into the MCM-41 hosts.

Power X-ray diffraction analysis: Fig. 2 shows XRD curves represented for three samples, namely, MCM-41, (MCM-41)-ASApA-(I), (MCM-41)-ASApA-(II) at 0.4-10.0°, from which one can see that in curve A, B and C, (100

diffraction peaks of the MCM-41 molecular sieve have all emerged with great intensity. Curve A even shows three relatively weaker diffraction peaks, corresponding to (110), (210) and (220), which are clearly visible. This shows that the prepared MCM-41 molecular sieve has good quality¹⁰. In Fig. 2, compared with curve (A), curve (B) contains diffraction peaks of decreased intensity while the diffraction intensity in curve (C) decreases even more, even that diffraction peak (220) disappeared. This shows that ASApA molecules entered into the molecular sieve, leading to a lowered diffraction contrast. The more ASApA molecules entered, the more impact formed on the diffraction.

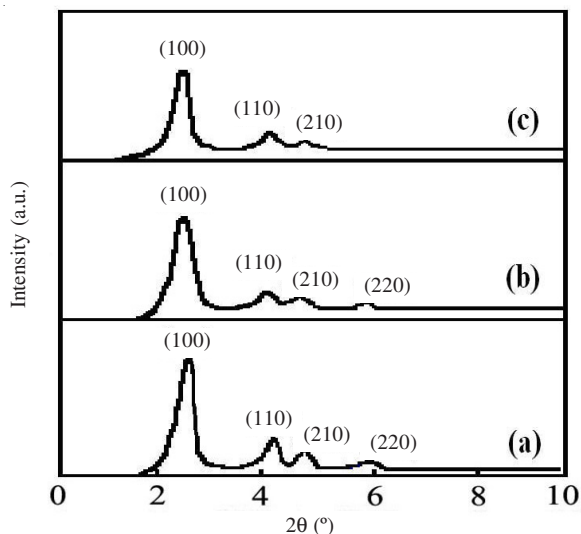
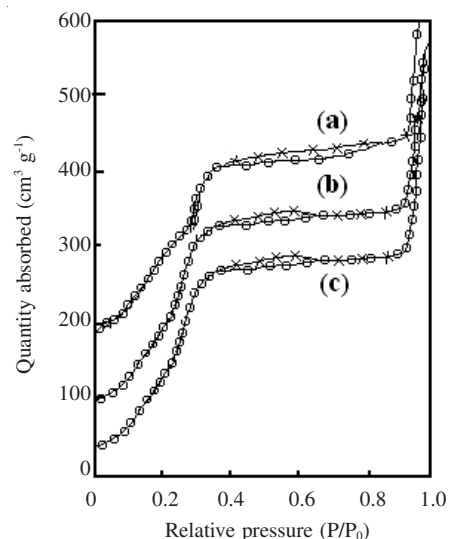


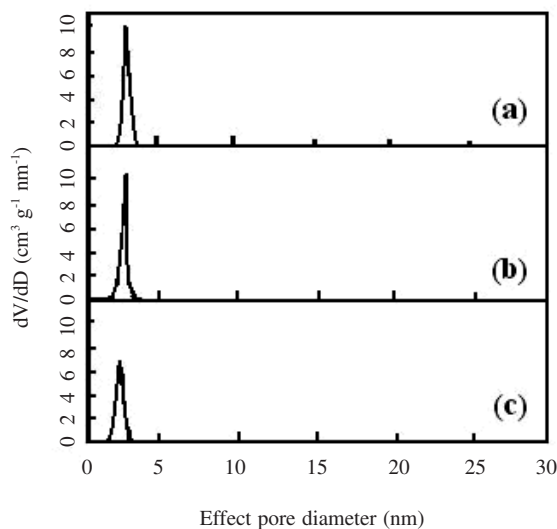
Fig. 2. XRD patterns of the samples: (a) MCM-41; (b) (MCM-41)-ASApA-I; (c) (MCM-41)-ASApA-II

Low temperature N₂ adsorption-desorption isotherms:

Fig. 3 is the N₂ adsorption-desorption isotherms and pore size distribution patterns at the low temperature of 77 K corresponding to sample MCM-41, (MCM-41)-ASApA-I and (MCM-41)-ASApA-II. From Fig. 3 (A), it can be seen that N₂ adsorption-desorption isotherms of three samples belong to mesoporous material isotherms with hysteresis loop of H1, which proves that they have characteristics of mesoporous materials of one-dimensional cylindrical pore. Mesoporous materials have single pore size distribution, whose adsorption of nitrogen at low temperature can be divided into three phases: the first phase provides smaller pressure and nitrogen molecules are adsorbed on pores in monolayer, which makes the absorption curve flattening; the second stage provides the medium pressure range. Due to the capillary cohesion of nitrogen molecules adsorbed on pores in monolayer and multilayer adsorption, the adsorption capacity increases rapidly with increased pressure. In third stage, the adsorption gradually reaches saturation so that adsorption capacity slowly increases with increased pressure. The more the sudden jump pressure occurs in the medium pressure range, the larger the sample aperture is. On the other hand, in the phase of sudden jump, the steep degree of the curve can be used to measure whether the sample aperture is uniform. The large rangeability (large slope) represents good pore uniformity, that is, pore size distribution is narrow.



(A)



(B)

Fig. 3. (A) Low temperature N₂ adsorption-desorption curves (B) pore size distribution patterns: (a) MCM-41; (b) (MCM-41)-ASApA-I; (c) (MCM-41)-ASApA-II

From Fig. 3 (A), it can be seen that N₂ adsorption-desorption isotherms and the hysteresis loop of MCM-41, (MCM-41)-ASApA-I and (MCM-41)-ASApA-II at low temperature are similar to each other, indicating that structures of MCM-41 mesoporous pore were not destroyed by the introduction of ASApA. From the perspective of branches of adsorption and desorption, three samples have generated three phases, very consistent with the adsorption characteristics of mesoporous materials. First of all, when the relative partial pressure changes from 0-0.40, the adsorption curve is more gentle and then N₂ adsorption-desorption curve of curves (A) emerges into sudden jump when relative partial pressure enters a medium-pressure zone from 0.40-0.82; while the sudden jump of curve B and C occurs when relatively partial pressure changes between 0.40-0.62 and finally, curve (A) tends to be gentle when the adsorption capacity of the relative partial pressure between 0.82-1.00 increases with the increased relative pressure. When the relative partial pressure reaches 0.62, the increment of curve B and C also tends to be gentle, indicating

that the sample adsorption gradually reaches saturation. Compared with non-assembled MCM-41, samples (MCM-41)-ASApA-(I) and (MCM-41)-ASApA-(II) have smaller sudden jump ranges of the relative partial pressure. That is because the guest materials of the samples, through the process of assembling, entered into the molecular sieve pores and occupied part of the pore volume, leading to that the relative partial pressure of its occurrence of adsorption has a smaller range than that of the MCM-41 sample.

Fig. 3(B) is pore size distribution patterns of the samples MCM-41, (MCM-41)-ASApA-(I) and (MCM-41)-ASApA-(II), indicating that the pore sizes of (MCM-41)-ASApA-(I) and (MCM-41)-ASApA-(II) have been reduced compared with that of the non-assembled sample MCM-41, which is in line with the reducing pressure ranges of breaking pressures of samples (MCM-41)-ASApA-(I) and (MCM-41)-ASApA-(II) in Fig. 3(A).

When integrated with XRD diagram of samples in Fig. 2, structural parameters can be calculated and shown in Table-1. Table-1 shows that the sample (MCM-41)-ASApA-(I), compared with MCM-41, has lower parameters of surface area, pore size and pore volume, etc., while for the (MCM-41)-ASApA-(II) with higher ASApA level the parameters are reduced more significant because ASApA was assembled into the molecular sieve and occupied its pores. In addition, pore walls of (MCM-41)-ASApA-(I) and (MCM-41)-ASApA-(II) have been increased compared with that of MCM-41, because the ASApA has occupied the inner surface of pore walls and adsorbed on them, thickening those pore walls, which also proves the ASApA have been successfully assembled into the pore of the molecular sieves. In composite materials, ASApA molecules mainly combined with the inner surface of pores by vander Waals' force.

To further study the host-guest nanocomposite materials, we use the normalized surface area for quantitative calculation according to Table-1 in order to determine the shapes of guest dye molecules in mesoporous molecular sieve pores. The formula of normalized surface area (NSA) is as follows¹⁷:

$$NSA = \frac{SA_1}{1-y} \times \frac{1}{SA_2}$$

In the above formula, the mass fraction of guest dye molecule in the composite material is set as y , while SA_1 and SA_2 represent surface areas of (MCM-41)-ASApA composite material and nano MCM-41 molecular sieve, respectively. According

to calculation results of normalized surface area, guest material usually has three patterns of distribution.

First of all, when $NSA \ll 1$, it shows that the guest material presents as relatively large graininess in the composite. Due to the entering of such graininess, molecular sieve generates pore blocking with the performance of a rapidly decreased pore volume, specific surface area and pore size of composite material in relation to the main molecular sieve (Fig. 4).

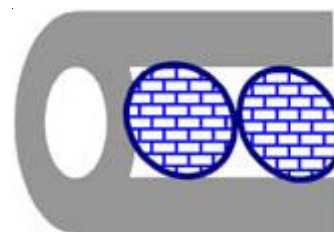


Fig. 4. Guest phase assembly type I in molecular sieve channel

Secondly, when $NSA \approx 1$, this shows that the guest material has generated an amorphous layer in the pore of host material, which closely covers the inner surface of the pores of molecular sieve (Fig. 5). Since these particles are attaching to inner surface of the pores of molecular sieve, a new surface is formed which only covers the original surface. Therefore, the normalized surface area value of such material is close to 1.

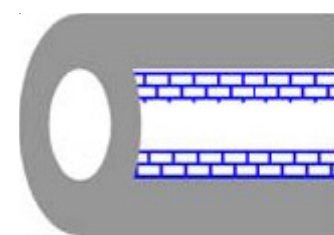


Fig. 5. Guest phase assembly type II in molecular sieve channel

Thirdly, when $NSA > 1$, this shows that the guest material generates very small nanocrystals (Fig. 6). These nanocrystals, scattered over the inner and outer surface of molecular sieve, have smaller nanoparticle sizes than the pore size, so that specific surface area of the composite material will not generate clogging pores due to the introduction of guest material. Moreover, the specific surface area will be increased due to it.

Through calculation, NSA value of (MCM-41)-ASApA-(I) is 0.83, while NSA value of (MCM-41)-ASApA-(II) is 0.76,

TABLE-1
PORE STRUCTURE PARAMETERS OF THE SAMPLES

Sample	Crystal face spacing/ d_{100} (Å)	Unit cell parameter/ a_0^a (Å)	BET surface area (m^2/g)	Pore volume ^b (cm^3/g)	Pore size ^c (Å)	Wall thickness ^d (Å)	Content of ASApA (wt. %)
MCM-41	33.4	38.5	961	0.566	22.9	15.6	0
(MCM-41)-ASApA (I)	35.8	41.3	789	0.530	21.6	19.7	0.82
(MCM-41)-ASApA (II)	37.5	43.4	706	0.363	21.3	22.1	1.93

a: Unit cell parameter, $a_0 = \frac{2}{\sqrt{3}}d_{100}$, b: BJH adsorption cumulative volume of pores, c: Pore size calculated from the adsorption branch, d: Wall thickness calculated by (a_0 - pore size).

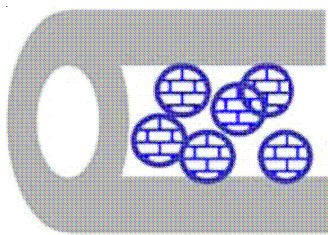


Fig. 6. Guest phase assembly type III in molecular sieve channel

indicating that the guest dye molecules form an amorphous layer in the pore of MCM-41 molecular sieve (Fig. 6) and closely cover the inner surface of the pores of molecular sieve. With the increase in assembly concentration of the guest, NSA decreases because there are more guests entering into the pores of host molecular sieve and blocking pores. This resulted in lowered specific surface areas and pore volumes of composite materials, which matches results of the adsorption-desorption experiment in Table-1.

Scanning electron microscopic images: Fig. 7 shows scanning electron microscopic images for the sample (MCM-41)-ASApA-(II) containing 2.93 % of ASApA. It can be seen that the particles are spherical and have a size of uniformity. The particle size is 115 ± 10 nm and the particle surface has no aggregated ASApA molecules.

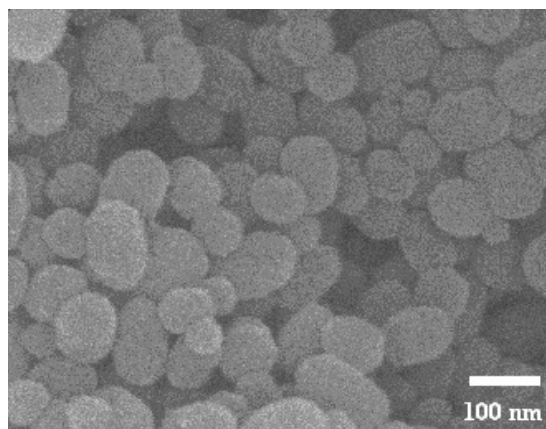


Fig. 7. Scanning electronic microscopic images of (MCM-41)-ASApA

Raman spectra: Fig. 8 shows Raman spectra of the samples, where curve (A) represents Raman spectrum of the nano MCM-41. Four characteristic peaks can be seen in the figure located at 495, 607, 810 and 980 cm^{-1} , respectively. The characteristic peak of 980 cm^{-1} is generated from Si-OH group of the molecular sieve, while the characteristic peak of 810 cm^{-1} is generated from Si-O-Si symmetric stretching vibration. The characteristic peak of 607 cm^{-1} proves that Si-O bridge bond exists in mesoporous molecular sieve. The characteristic peak of 495 cm^{-1} is relatively wider because of superimposed vibration of multi-membered ring (such as three-membered ring, four-membered ring, etc.). Curves B and C represent Raman spectra curves of the host-guest composites. Compared with curve (A), curves B and C have weaker intensity of characteristic peaks. It is because after the guest dye molecules enter into the molecular sieve, its surface free-OH generates bonding reaction, leading to changed molecular rigidity that affects the molecular vibrations of the host materials, thus

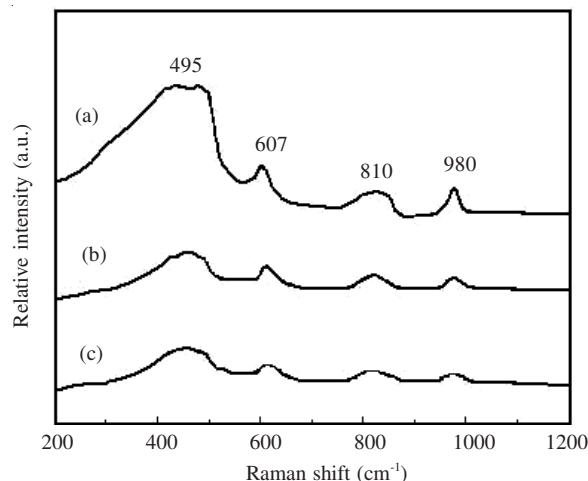


Fig. 8. Raman spectra: (a) MCM-41; (b) (MCM-41)-ASApA-(I); (c) (MCM-41)-ASApA-(II)

reducing the original intensities of Raman spectra of the host materials. The mass fraction of host of composite material represented by curve C is higher than that of curve B. Thus, after comparison, the intensity of spectral peak of curve C is weaker than that of curve B, which, from the side perspective, proves that the guest dye molecules have entered the host molecular sieve.

UV-Visible solid diffusion reflection absorption spectra: Fig. 9 shows UV-visible solid diffusion reflection absorption spectra, from which it can be seen that the nanometer MCM-41 molecular sieve has not absorption peak in the visible-UV area, while ASApA has two absorption peaks 200-800 nm range. Two absorption peaks are located at 330 and 709 nm. Curve B in Fig. 8 shows the absorption curve of the sample (MCM-41)-ASApA-(I). As the ASApA has a lower level in the composite, absorption peak does not appear within the scope of area. Curve C represents the absorption curve of the sample (MCM-41)-ASApA-(II). Compared with the absorption curve of the nanometer MCM-41 molecular sieve, the two absorption peaks are located at 296 and 671 nm, which are

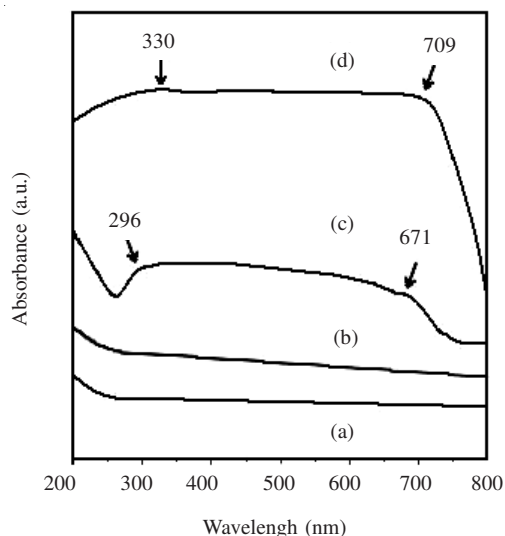


Fig. 9. UV-Vis solid diffuse reflection absorption spectra: (A) MCM-41; (B) (MCM-41)-ASApA-(I); (C) (MCM-41)-ASApA-(II); (D) ASApA

caused by assembling ASApA into the pores of the molecular sieve. However, the absorption peak position has generated hypochromatic shift, compared with the two absorption peaks of ASApA with the range of 34 and 38 nm, because the nano-MCM-41 molecular sieve has effects of quantum confinement on guest materials, increasing the width of forbidden gap. This results in increased energy needed by electron transition of composite materials with the performance of the hypochromatic shift of absorption peaks.

Luminescence spectra: Fig. 10 shows excitation-emission spectra of (MCM-41)-ASApA. The MCM-41 mesoporous molecular sieve itself does not have light-emitting property. After the guest material ASApA was assembled into MCM-41 channels, the host-guest composite material possesses light-emitting properties at 466 nm. Under normal conditions, the dye molecules will assemble in the solution. After agglomeration, the excitation energy of dye molecules can easily be released through thermal relaxation rather than effectively to be turned into luminous energy. Whatever the concentrations of dye molecules in solution are, the agglomeration will occur, so that the performance of their optical activity can not be truly reflected. The dye molecules assembled into the mesoporous pores are farther parted, thereby having weakened interactions, which makes the contribution of fluorescence quenching relatively small. Large surface area of porous silica provides adequate space for the dye molecules embedded in it, keeping certain distance among dye molecules, which enables most of ASApA molecules to attach to the pore wall of mesoporous molecular sieve in the form of monomer. Thus, agglomeration of dye molecules can be reduced. The nanoscale pores of mesoporous molecular sieve limit the activity space of ASApA molecules. This weakens interaction between dyes molecules filled in the mesoporous pores. Agglomeration is difficult to form in the pores thus showing similarities with the single molecule light-emitting properties. In MCM-41 mesoporous silica molecular sieve, ASApA dyes basically exist in the form of monomers. When it is exposed in exciting light, the dye molecules will jump from ground state to levels with different quantum numbers. However, due to the limit

of pore size, the activities of dye molecules are bounded, thus weakening the rotational energy of molecules greatly. This leads to the reduced non-radiative transition caused by rotational relaxation. In the end, dye molecules jump from vibrational levels with different excitation states to vibrational levels with different ground states, letting off fluorescence.

In addition, since -OH exists in the inner surface of pores of the molecular sieve, it can improve the rigidity of planar molecules together with ASApA molecular bonding. The molecular fluorescence with a rigid planar structure has a high yield because it is turned rigidity by base materials, making the guest dye molecules in the solid substrate surface show optical properties that do not exist in the solution and powder state. Inorganic host can transfer most of its absorbed ultraviolet energy to the organic guest molecules, thereby increasing the excitation energy and a corresponding increase in fluorescence intensity. The host-guest composite materials (MCM-41)-ASApA have potential use in the domain of sensor, light-emitting devices and laser part materials.

Conclusion

In this study, (MCM-41)-ASApA host-guest nanocomposites were prepared and the guest material was successfully assembled into pores of the host molecular sieve. The (MCM-41)-ASApA composite materials present luminous property at 466 nm. They have the potential use in the domain of sensor, light-emitting devices and laser part materials.

ACKNOWLEDGEMENTS

The authors express their thanks to Sino-US international cooperation project for support. The project number was 2008DFA40270,270330 (KYC -MX- XM-2009- 001).

REFERENCES

1. C.T. Kresge, M.E. Leonowicz, W.J. Roth, J.C. Vartuli and J.S. Beck, *Nature*, **359**, 710 (1992).
2. C.Q. Li, H.T. Zhang, G.D. Sun, Y.R. Sun and F.Y. Li, *Acta Petrolei Sinica*, **24**, 646 (2008).
3. R. Cui, X.Q. Liu and J.H. Shan, *Chem. Engin. Oil Gas*, **37**, 279 (2008).
4. L.L. Feng, W. Zhao, Y. Liu, L. Jiao and X.G. Li, *Acta Phys.-Chim. Sinica*, **25**, 1347 (2009).
5. L.X. Guan, J.P. Li, X.Z. Wang, N. Zhao, W. Wei and Y.H. Sun, *Petrochem. Tech.*, **26**, 1282 (2007).
6. N. Bai, P. Zhang, Y.H. Guo, S.G. Li, W.Q. Pang, W. Luo and G.T. Zou, *Chem. Res. Chin. Univ.*, **23**, 786 (2002).
7. F.F. Wang and Q.S. Li, *J. Qufu Normal Univ.*, **29**, 49 (2003).
8. D. Zhao, W.P. Qin, J.S. Zhang, G.S. Qin, Z.F. Wu, H.Q. Liu, H.Y. Lin and W. Xu, *Chin. J. Lumin.*, **24**, 637 (2003).
9. F. Yang, J.H. Rong, Y.L. Liu, D.S. Yuan and J.X. Zhang, *J. Function. Mater.*, **36**, 575 (2005).
10. Q. Cai, Z.S. Luo, W.Q. Pang, Y.W. Fan, X.H. Chen and F.Z. Cui, *Chem. Mater.*, **73**, 258 (2001).
11. J.M. Pan, Z.J. Li, Q.Y. Zhang and G.Z. Fan, *New Chromogenic Reagents and their Application in Spectrophotometry*, Beijing: Chemical Industry Press, 54 (2003).
12. J. Xu, C.P. Wei and C.X. Chi, *J. Jilin Univ.*, **37**, 1323 (2007).
13. Y. Chen, X.T. Li, L.M.N. Gu, N. Li, G.S. Zhu and S.L. Qiu, *Chem. J. Chin. Univ.*, **27**, 397 (2006).
14. Q.Z. Zhai and C.Y. Mei, *Hydrometallurgy (China)*, **4**, 56 (1998).
15. J.C.P. Broekhoff and J.H. Deboer, *J. Catal.*, **10**, 307 (1968).
16. S. Brumauer, P.H. Emmett and E. Teller, *J. Am. Chem. Soc.*, **60**, 309 (1938).
17. L. Vradman, M.V. Landau, D. Kantorovich, Y. Koltypin and A. Gedanken, *Micropor. Mesopor. Mater.*, **79**, 307 (2005).

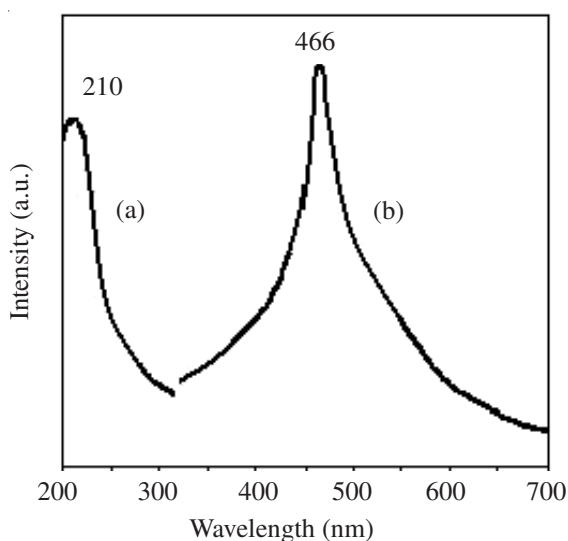


Fig. 10. Luminous spectra of (MCM-41)-ASApA: (a) excitation spectrum; (b) emission spectrum